

Fig. S1 KMC simulation flow chart.

Parameter	Value
resistances between empty site (R_{high})	$10^6 \Omega$
resistances between metal atom (R_{low})	5Ω
frequency factor for transition probability (F_{freq})	10^{13} s^{-1}
Activation energy for volume diffusion (E_a)	0.5 eV
Activation energy for oxidation ($E_{a,\text{ox}}$)	0.45 eV
Activation energy for reduction ($E_{a,\text{Red}}$)	0.5 eV
Activation energy for surface diffusion ($E_{a,\text{Srf}}$)	0.5 eV
Activation energy for desorption ($E_{a,\text{Des}}$)	0.45 eV
Distance between adjacent transition size (h)	0.5 nm
Electric Susceptibility (χ)	3.2

Fig. S2 Simulation parameters for metal(Ag)-atom-filaments in the solid-electrolyte(Cu_xO) of a CBRAM.

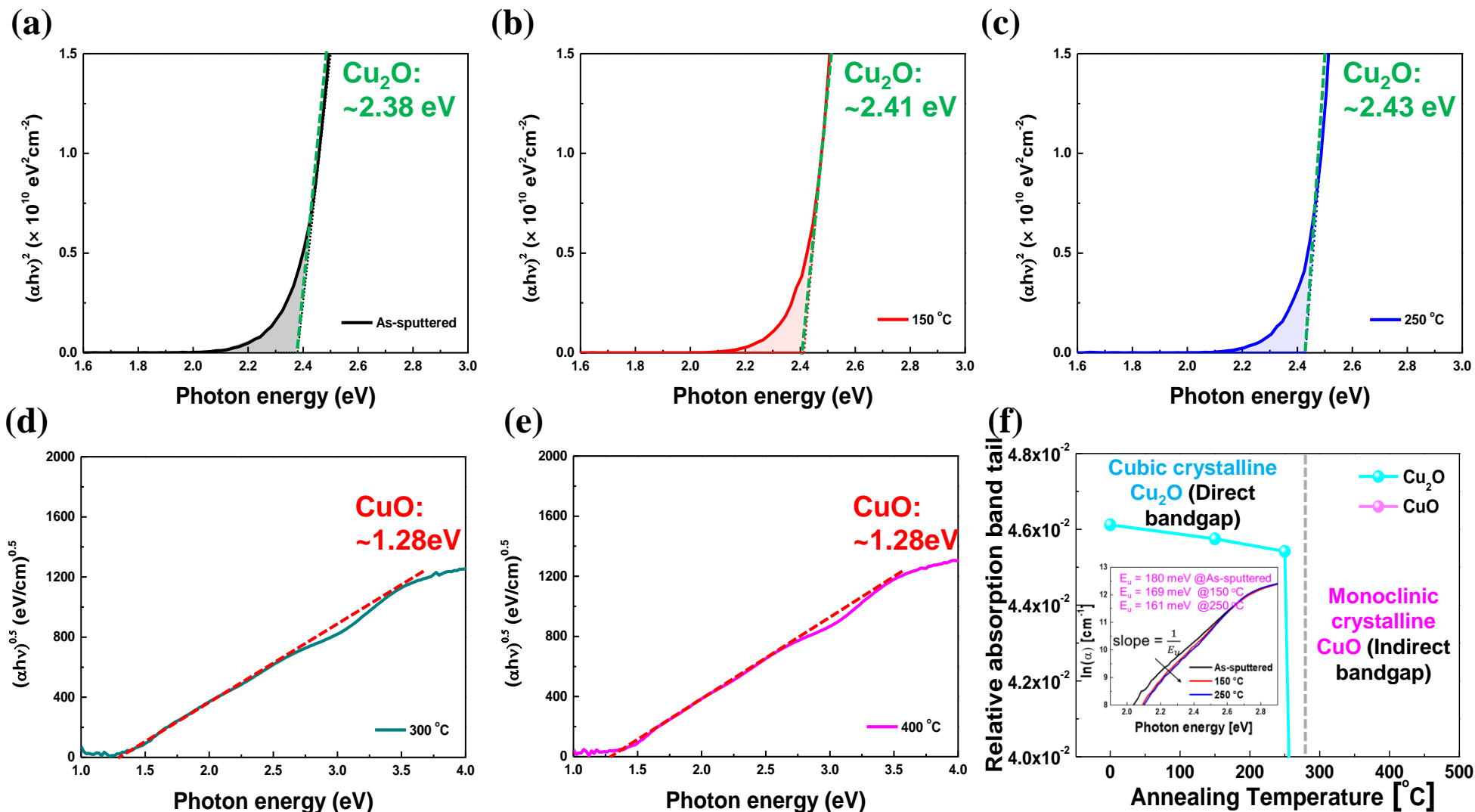


Fig. S3 Dependency of Tauc plot fitting for calculating bandgap energy on different ex-situ annealing temperatures for the Cu_xO solid-electrolytes: (a) as-sputtered, (b) 150 °C, (c) 250 °C (d) 300 °C, (e) 400 °C, and (f) relative absorption band tail (Urbach energy). Relative absorption band tail was measured an integrated area less than optical energy bandgap

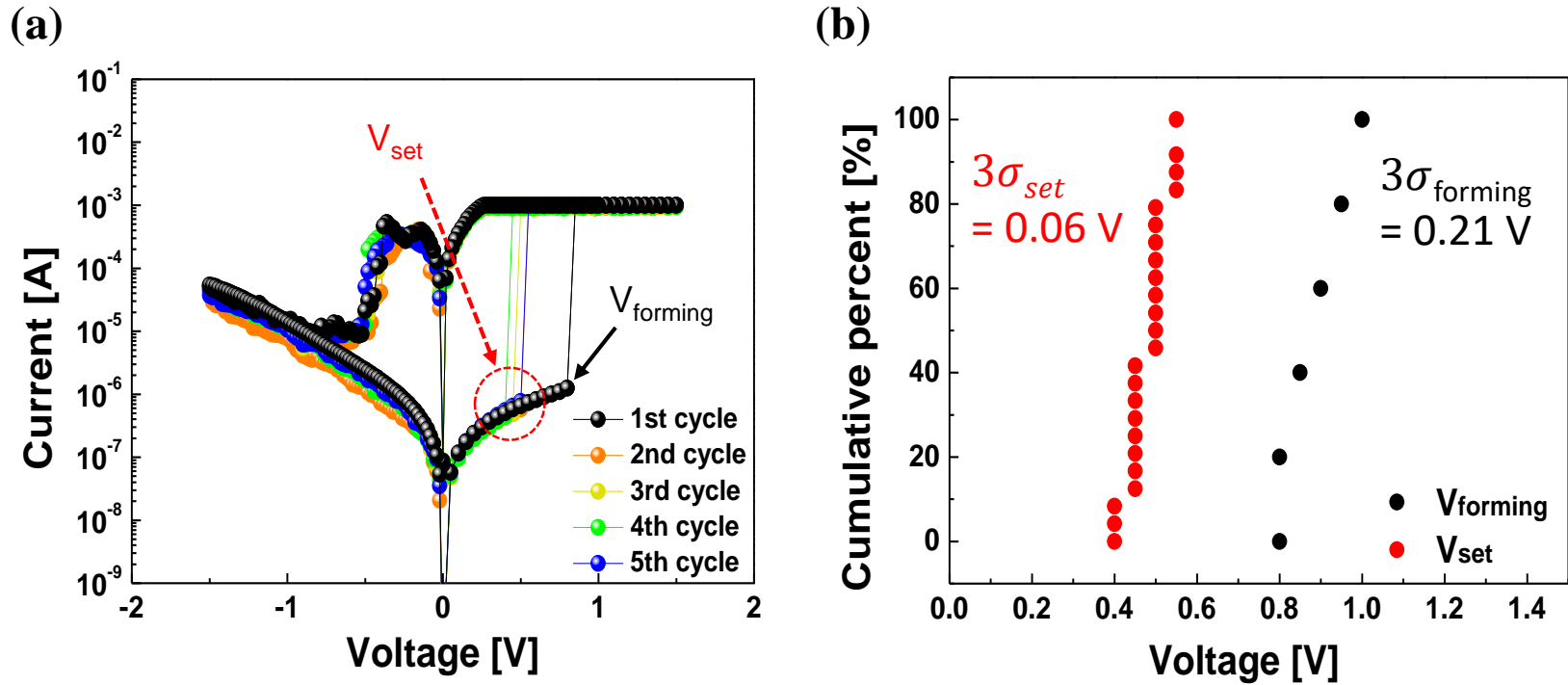


Fig. S4 Distribution of set voltage (V_{set}) and forming voltage ($V_{forming}$) for the CBRAM cells annealed at 300 °C for 30 min [Fig. 2d of manuscript]. I-V curves were measured 4 times after a forming per a CBRAM memory-cell. In addition, 6 different CBRAM memory-cells were estimated so that V_{set} of 24 times and $V_{forming}$ of 6 times were measured. The 3σ (standard deviation: 99 %) of V_{set} and $V_{forming}$ were 0.06 and 0.21 V, respectively, as shown in Fig. S4b. Moreover, the difference between maximum V_{set} and minimum $V_{forming}$ was ~ 0.2 V. As a result, the $V_{forming}$ could be obviously distinguished from V_{set} .

Holding time after finishing the top electrode deposition	Diffusion time (s)	Diffusion length (m)
1 hour	3,600	1.83×10^{-12}
1 day	86,400	8.99×10^{-12}
1 month	2,592,000	4.92×10^{-11}

Fig. S5 Diffusion length depending on the holding time of top electrode deposition. Ag atoms are diffused into the Cu_xO solid-electrolyte during Ag-atom electrode sputtering since the sputtering power is DC 30 Watt. After Ag-atom electrode sputtering, Ag atoms can be diffused only 8.99×10^{-12} m at room temperature for 1 month since diffusivity(D) of Ag atoms is 9.36×10^{-24} cm^2/sec , as shown in below our calculation table. In addition, the electrical properties of all CBRAM cells were estimated within 1 day. Thus, the Ag-atom depth profile in the Cu_xO solid-electrolyte is determined by sputtering of the Ag-atom electrode rather than the Ag-atom diffusion at room temperature. The Ag-atom diffusivity in the Cu_xO solid-electrolyte was calculated by reference [J. Phys. Chem. Solids 45, 3, 295-298 (1984)], as described in equation (1)

$$D = (D_{\text{Ag}})_0 \exp(-Q_{\text{Ag}}/RT) \quad (1)$$

where $(D_{\text{Ag}})_0 = 2.35 \times 10^{-3}$ cm^2/sec , $Q_{\text{Ag}} = 28.00$ kcal/mole, and $R = 1.987 \times 10^{-3}$ kcal \cdot K $^{-1}$ \cdot mol $^{-1}$ and the Ag-atom diffusivity in the Cu_xO solid-electrolyte was calculated at 300 K. As a result, $D(@300 \text{ K})$ was 9.36×10^{-24} cm^2/sec . The diffusion length of Ag atoms in the Cu_xO solid-electrolyte was calculated by using \sqrt{Dt} .

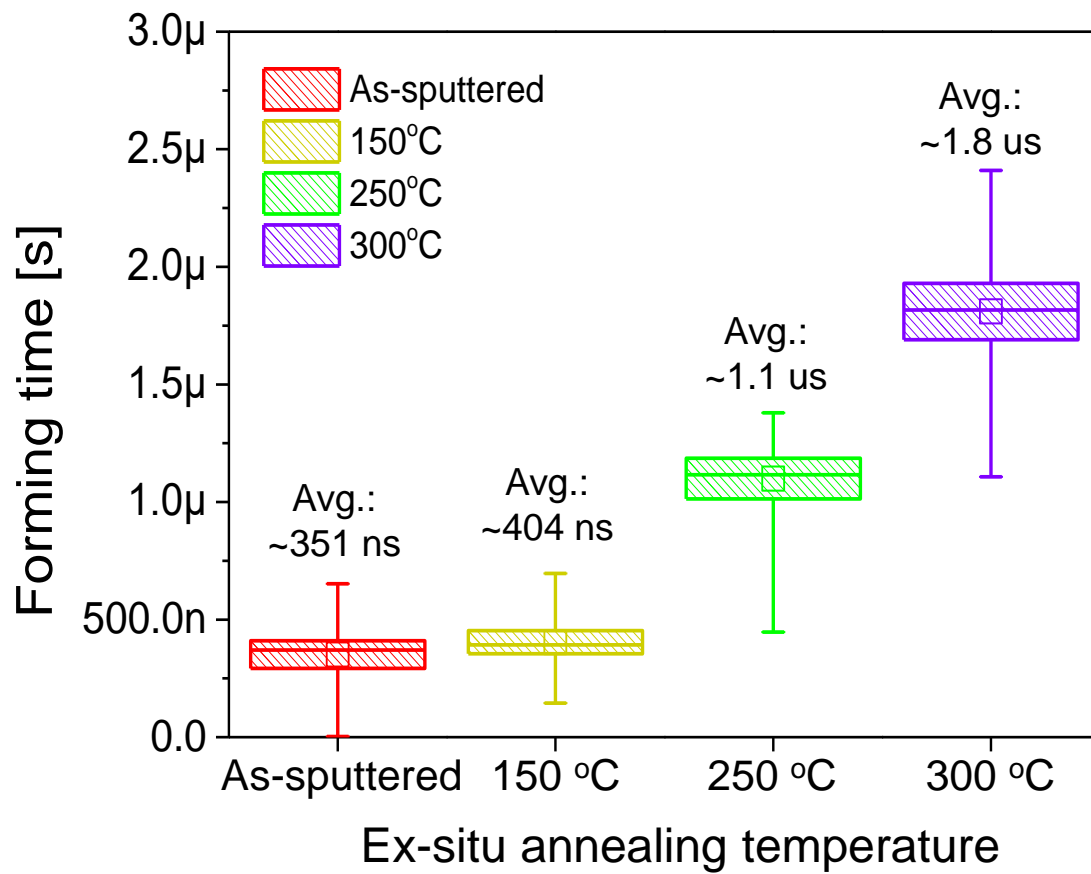


Fig. S6 Dependency of electro-forming time on ex-situ annealing temperature.

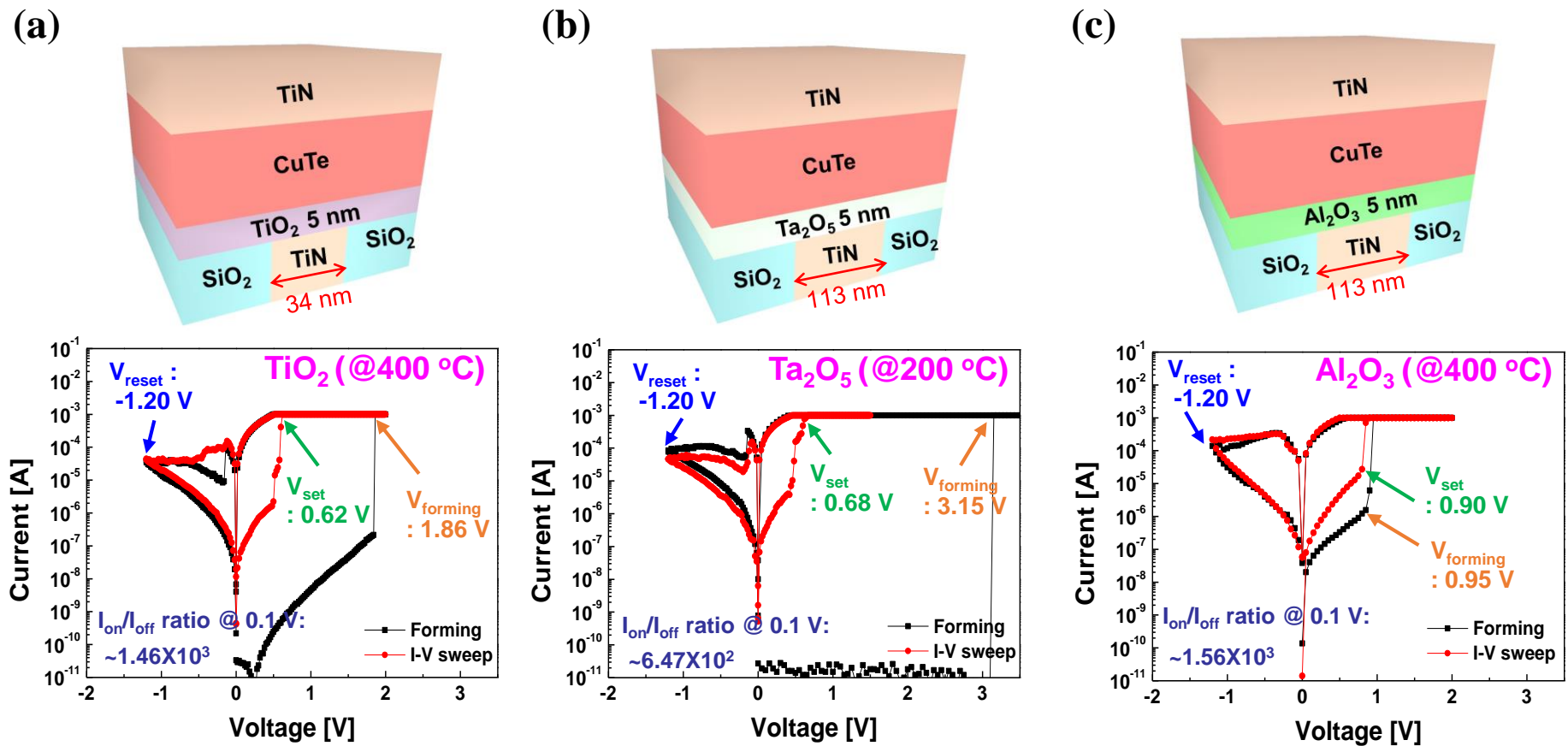


Fig. S7 Dependency of solid-electrolyte materials on CBRAM performance. (a) TiO₂ solid-electrolyte based CBRAM having 34-nm-diameter memory-cell size, annealed at 400 °C for 30 min, (b) Ta₂O₅ solid-electrolyte based CBRAM having 113-nm-diameter memory-cell size, annealed at 200 °C for 30 min, and (c) Al₂O₃ solid-electrolyte based CBRAM having 113-nm-diameter memory-cell size, annealed at 400 °C for 30 min. To form metallic-atom(Cu)-filaments in a solid-electrolyte, the CuTe electrode was used for metallic-atom source. All solid-electrolyte material showed a typical CBRAM behavior. In particular, both TiO₂ and Ta₂O₅ solid-electrolyte could not achieve forming-free but Al₂O₃ solid-electrolyte performed forming-free. Fig. S7 indicates that the forming-free achievement strongly depends on the solid-electrolyte materials, ex-situ annealing temperature, and memory-cell size.